OBSERVING GAP FORMATION IN THE DUST LAYER OF A PROTOPLANETARY DISK

Jean-François Gonzalez[1], Sarah Maddison[2], Laure Fouchet[3], Christophe Pinte[4], François Ménard[4], Guillaume Laibe[5]

[1] Centre de Recherche Astrophysique de Lyon, Université de Lyon, France
[2] Centre for Astrophysics and Supercomputing, Swinburne University of Technology, Melbourne, Australia
[3] Physikalisches Institut, Universität Bern, Switzerland
[4] Laboratoire d'AstrOphysique de Grenoble, Université Joseph Fourier, Grenoble, France
[5] Center for Stellar and Planetary Astrophysics, Monash University, Australia

ABSTRACT

We numerically model the evolution of dust in a protoplanetary disk using a 3D, two-phase (gas+dust) smoothed particle hydrodynamics (SPH) code, which is non self-gravitating and locally isothermal. The gas and dust interact via aerodynamic drag, allowing the evolution of the dust distribution in protoplanetary disks to be followed. In this work, we present the evolution of a disk comprising 1% dust by mass in the presence of an embedded planet is a typical Classical T Tauri star (CTTS) disk. We then vary the grain size (100 µm to 10 cm) and planetary mass (0.1 to 5 M_J) to see how they affect the resulting disk structure. We find that gap formation is much more rapid and striking in the dust layer than in the gaseous disk and that a system with a given stellar, disk and planetary mass will have a completely different appearance depending on the grain size and that such differences will be detectable in the millimeter domain with ALMA. Dust accumulates at the edges of the planetary gap where its density exceeds that of the gas phase. In new simulations including grain growth, we find that particles grow most efficiently in these high density regions. Gap edges therefore appear as potential sites for the formation of additional planets.

INTRODUCTION

Gaps carved by planets in gas disks have been well studied theoretically and numerically (see Papaloizou et al. 2007 for a review). More recent work (Paardekooper & Mellema 2006, Fouchet et al. 2007) has shown that gaps are more pronounced in the dust layer of a Minimum Mass Solar Nebula (MMSN) disk. Here we study the formation of gaps in dusty CTTS disks, motivated by their observability with ALMA which has been shown by Wolf & D'Angelo (2005) assuming perfect mixing of gas and dust. We consider dust grains in the size range where gas drag has the strongest effect on their dynamics and which ALMA will be able to detect.

SIMULATIONS

We use our 3D, two-phase (gas+dust), non self-gravitating, locally isothermal SPH code (Barrière-Fouchet et al. 2005) to model the evolution of dust grains under the influence of gas drag in the Epstein regime.
Our standard disk orbits a 1 $M_\odot$ star, has a mass M_{disk}=0.02 $M_\odot$ and a viscosity α≈0.01, and extends from 4 to 160 AU. It contains 1% of 1 mm-sized dust grains by mass and a 5 M_J planet at 40 AU. The simulations include 400,000 SPH particles and are evolved for 100 planet orbits (≈26,000 yr). We vary the grain size s (100 µm to 10 cm) and planet mass M_p (0.1 to 5 M_J). In a final run, we include grain growth from an initial size of 10 µm.

PLANET GAPS IN THE DUST LAYER OF DISKS

Our previous work on planet-less disks (Barrière-Fouchet et al. 2005) showed that tiny grains are coupled to the gas and follow its evolution, while large grains are decoupled and follow their own orbits. For intermediate sizes around s_{opt} (optimal size depending on the nebula parameters, 1 mm-1 cm for our CTTS disk), gas drag is most efficient and grains settle to the midplane and migrate radially.

Gap opening depends on the disk scale height H (Crida et al. 2006) and is easier in the settled dust layer than in the flared gas disk, as seen in Figs. 1 and 2. Gaps are deeper and wider for (1) larger grains (with smaller H) and (2) more massive planets. Larger planet masses are required to open a gap in the gas phase than in the dust. While a 0.5 M_J planet only slightly affects the gas phase, it carves a deep gap in the dust. Grains can be seen trapped in corotation only for the most massive 5 M_J planet (see Fouchet et al. 2010 for details).

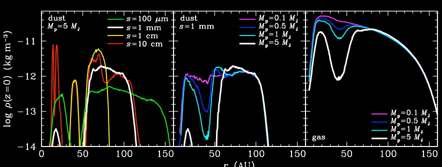

Fig. 1: Azimuthally averaged density of gas and dust in the disk midplane for various s and M_p.

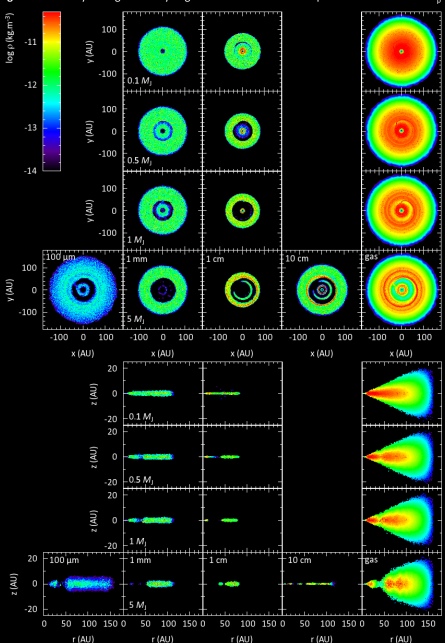

Fig. 2: Face-on (top) and edge-on (bottom) views of the gas and dust densities for CTTS disks with planets of 0.1 to 5 M_J and grain sizes from 100 µm to 10 cm.

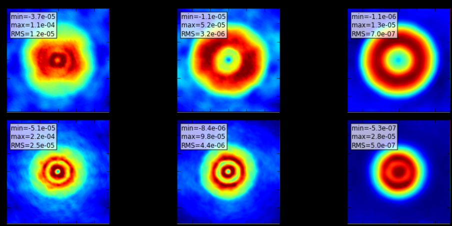

Fig. 3: ALMA synthetic images of the CTTS disk with a 1 M_J planet for λ=850, 1300 and 2700 µm, from left to right, for array configuration 20 (longest baseline ~ 4 km). Top: naïve well-mixed assumption. Bottom: self-consistently included aerodynamic drag.

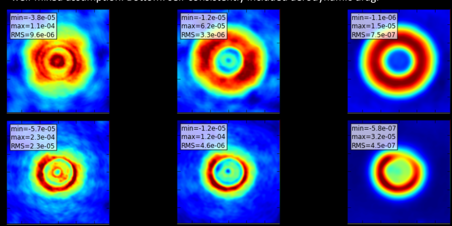

Fig. 4: Same as Fig. 3 for a 5 M_J planet.

SYNTHETIC IMAGES: PREDICTIONS FOR ALMA

Wolf & D'Angelo (2005) showed that gaps carved by 1 M_J planets should be detectable by ALMA up to 100 pc. However, they used 2D simulations of a planet in a gas disk and assumed that dust grains were perfectly mixed with the gas before performing 3D radiative transfer calculations to obtain synthetic images at the shortest ALMA wavelength (350 µm) and therefore the highest spatial resolution.

We use the dust distributions obtained from our 3D SPH simulations for each grain size as an input to the 3D radiative transfer code MCFOST (Pinte et al. 2006) to compute synthetic scattered light images at several ALMA wavelengths. We reconstruct a grain size distribution described by a power law of index -3.5. Outside the size range of our SPH simulations, small grains are assumed to be perfectly coupled to the gas and large grains are omitted because their contribution to scattered light at those wavelengths is negligible. We also compute images assuming grains of all sizes follow the gas in order to highlight the important effect of gas drag. The resulting synthetic images are then passed on to the CASA simulator for ALMA and are shown in Figs. 2 and 3 for array configuration 20 (longest baseline ~ 4 km). They reproduce the decreasing spatial resolution as wavelength increases.

The images from the realistic case with aerodynamic drag (bottom row of Figs. 3 and 4) display notable features. The extent of the disk varies with wavelength, reflecting the location of different grain sizes in the disk (as grains with sizes closest to the wavelength contribute the most). The disk asymmetry caused by the spiral wave in the 5 M_J planet case is clearly visible and can provide a constraint on the angular position of the planet. Finally, the gap has a much higher contrast in the realistic case than in the naïve mixed case: it is deeper and its edges are denser and brighter. Even for the 1 M_J planet, it is still visible at the lowest resolution, whereas the naïve mixed case would only show a central hole. Gaps carved by lighter planets will therefore be much easier to detect than anticipated.

GRAIN GROWTH AROUND PLANET GAPS

We ran a new simulation for our standard configuration, this time letting grains grow from a uniform initial size of 10 µm. Dust particles are assumed to stick perfectly upon collision and never shatter, following the prescription of Stepinski & Valageas (1997), which we implemented in our SPH code. In previous calculations for planet-less disks, we showed that, under the combined effects of gas drag and growth, dust grains experience 3 phases: settling and growth, rapid migration with little growth, and growth with little migration in the dense inner disk (Laibe et al. 2008, see also poster P11:2 by Crespe et al., this conference).

The presence of a planet alters the behavior of the grain population:
• In the dense region interior to the planet, grains grow rapidly and, when they reach s_{opt} (≈1 cm in that region, Fig. 5b), fall into the star. As more grains migrate in this region, they grow past s_{opt}, decouple from the gas, and continue to grow without migrating (Fig. 5c-d).
• Grains near the planet's orbit first grow rapidly but as the gap forms, the density decreases and the grains left in corotation with the planet stop growing (Fig. 5c-d).
• Exterior to the planet, grains behave similarly to the planet-less case: they grow as they settle (Fig. 5b), then migrate when they reach s_{opt} ("horizontal branch" in Fig. 5c) and pile up at the gap outer edge (Fig. 5d). Grains migrating outwards from the gap contribute to the high density there, which promotes an efficient growth.

The two high-density regions at the gap edges (Fig. 6), where growth is enhanced, appear are potential sites for the formation of planetesimals.

In addition, gravitational instability may occur at the outer edge, where the Toomre (1964) parameter is Q≈1, and may trigger the formation of additional planets. This is not the case at the inner edge where Q≈10.

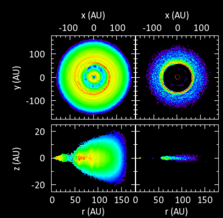

Fig. 6: Face-on (top) and edge-on (bottom) views of the gas (left) and dust (right) densities in the CTTS disk with a 5 M_J planet and grain growth.

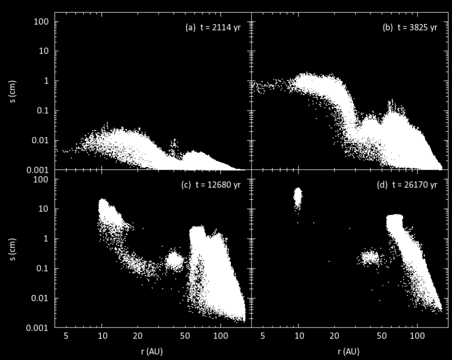

Fig. 5: Evolution of the size distribution of growing grains in the CTTS disk with a 5 M_J planet.

CONCLUSION

• Gaps are more striking and require a smaller planet mass to form in the dust phase than in the gas. They are wider and deeper for larger grains. These results confirm those of our MMSN study (Fouchet et al. 2007).
• The variety of structures seen for different s and M_p are visible in the synthetic images and future ALMA observations will be able to constrain both parameters. Gaps will be detectable for lighter planets than anticipated.
• When grain growth is included, it is most efficient in the high density regions at the gap edges, which appear as efficient sites for planetesimal formation.

REFERENCES

Barrière-Fouchet et al. 2005, A&A 443, 185
Crida et al. 2006, Icarus 181, 587
Fouchet et al. 2007, A&A 474, 1037
Fouchet et al. 2010, A&A 518, A16
Laibe et al. 2008, A&A 487, 265
Paardekooper & Mellema 2006, A&A 453, 1129
Papaloizou et al. 2007, PPV, 655
Pinte et al. 2006, A&A 459, 797
Stepinski & Valageas 1997, A&A 319, 1007
Toomre 1964, ApJ 139, 1217
Wolf & D'Angelo 2005, ApJ 619, 1114

ACKNOWLEDGEMENTS

This research was partially supported by the Agence Nationale de la Recherche (ANR) of France through contract ANR-07-BLAN-0221, and the Swinburne Special Studies Program. and the Swiss National Science Foundation through a Maria Heim-Voegtlin fellowship. Simulations presented here were run on the Swinburne supercomputer (http://astronomy.swin.edu.au/supercomputing) and the Fostino cluster at LAOG.